SANDIA REPORT
SAND2010-7734
Unlimited Release
Printed November 2010

A Revolution in Micropower: The Catalytic Nanodiode

J. Randall Creighton, Michael E. Coltrin, Jeffrey J. Figiel, Karen C. Cross, Daniel D. Koleske, Roger P. Pawlowski, Edwin J. Heller, Katherine H.A. Bogart, Eric Coker, Kevin C. Baucom

Prepared by
Sandia National Laboratories
Albuquerque, New Mexico 87185 and Livermore, California 94550

Sandia National Laboratories is a multi-program laboratory managed and operated by Sandia Corporation, a wholly owned subsidiary of Lockheed Martin Corporation, for the U.S. Department of Energy's National Nuclear Security Administration under contract DE-AC04-94AL85000.

Issued by Sandia National Laboratories, operated for the United States Department of Energy by Sandia Corporation.

Available to DOE and DOE contractors from
U.S. Department of Energy
Office of Scientific and Technical Information
P.O. Box 62
Oak Ridge, TN 37831

Telephone: (865) 576-8401
Facsimile: (865) 576-5728
E-Mail: reports@adonis.osti.gov
Online ordering: http://www.osti.gov/bridge

Available to the public from
U.S. Department of Commerce
National Technical Information Service
5285 Port Royal Rd.
Springfield, VA 22161

Telephone: (800) 553-6847
Facsimile: (703) 605-6900
E-Mail: orders@ntis.fedworld.gov
Online order: http://www.ntis.gov/help/ordermethods.asp?loc=7-4-0#online

SAND2010-7734
Unlimited Release
Printed November 2010

A Revolution in Micropower: The Catalytic Nanodiode

J. Randall Creighton, Michael E. Coltrin, Jeffrey J. Figiel, Karen C. Cross, Daniel D. Koleske,
Advanced Materials Sciences Department

Roger P. Pawlowski
Applied Math and Applications

Edwin J. Heller
Integrated Microdevice Systems

Katherine H. A. Bogart
Analytical Services Department

Eric Coker
Ceramic Processing and Inorganic Materials Department

Kevin C. Baucom
Center 1700 ES&H

Sandia National Laboratories
P.O. Box 5800
Albuquerque, NM 87185-1086

Abstract

Our ability to field useful, nano-enabled microsystems that capitalize on recent advances in sensor technology is severely limited by the energy density of available power sources. The catalytic nanodiode (reported by Somorjai's group at Berkeley in 2005) was potentially an alternative revolutionary source of micropower. Their first reports claimed that a sizable fraction of the chemical energy may be harvested via hot electrons (a "chemicurrent") that are created by the catalytic chemical reaction. We fabricated and tested Pt/GaN nanodiodes, which eventually produced currents up to several microamps. Our best reaction yields (electrons/CO_2) were on the order of 10^{-3}; well below the 75% values first reported by Somorjai (we note they have also been unable to reproduce their early results). Over the course of this Project we have determined that the whole concept of "chemicurrent", in fact, may be an illusion. Our results conclusively demonstrate that the current measured from our nanodiodes is derived from a thermoelectric voltage; we have found no credible evidence for true chemicurrent. Unfortunately this means that the catalytic nanodiode has no future as a micropower source.

Acknowledgements

The authors thank Robert K. Grubbs (Org. 2452) for depositing TiO_2 films by atomic layer deposition, and Alex Yun-Ju Lee (Org. 1816) for depositing TiO_2 films by reactive sputtering and sol-gel technique.

Contents

1. Introduction

Our ability to field useful, nano-enabled microsystems that capitalize on recent advances in sensor technology is severely limited by available power sources. Many such applications require power system volumes on the order of ½ cm^3 to 1 mm^3 in various form factors. Power density levels on the order of 1-10 microwatts/mm^2 are of greatest interest. In 2005-2006 a revolutionary type of micropower source was announced by Gabor Somorjai's research group (Berkeley); see **http://pubs.acs.org/cen/news/83/i15/8315notw1.html**, and refs. 1-5. They coined the term "catalytic nanodiode", and the device is simply a Schottky diode where the metal contact is made of an ultrathin (1-10 nm) catalytic metal, such as platinum or palladium. The source of energy is a catalytic reaction, in this case the CO oxidation reaction, CO + 1/2 $O_2 \rightarrow$ CO_2, which liberates ~2.9 eV of energy. If the metal is thin enough, many of the ballistic electrons created will live long enough to migrate to the semiconductor side (GaN or TiO_2) of the Schottky diode, yielding a "chemicurrent", see Fig. 1(a).

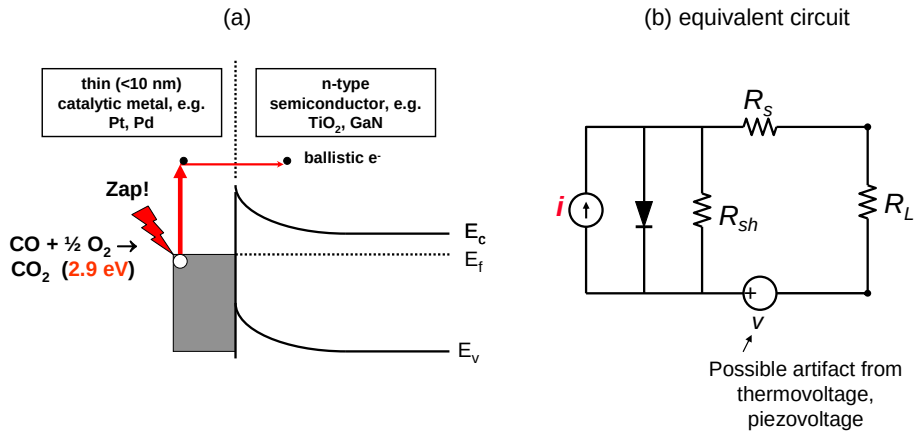

Figure 1. (a) Energy level diagram of the catalytic nanodiode, in this example with the CO oxidation reaction providing the energy source, (b) equivalent circuit diagram of nanodiode with chemicurrent-*i*

In an ambient of CO and O_2, Somorjai's best device produced a short-circuit current (I_{sc}) of 40 microamps (area ~ 1mm^2) at 80°C. By simultaneously measuring the CO_2 production rate Somorjai found that up to 3 electrons were created and harvested per 4 CO_2 produced, which would correspond to rather remarkable electron quantum efficiency of ~ 75%. The original goal of this project was to validate the concept, then use Sandia microsystem capabilities to

significantly advance the nanodiode technology for micropower applications. Unfortunately we failed to validate the basic concept of "chemicurrent" generation, and have instead concluded that the electronic signals are generated by a thermoelectric voltage. Heat liberated by the catalytic reaction leads to temperature gradients of ~1°C, which is sufficient to explain all experimental observations.

2. Nanodiode fabrication and electrical testing

We fabricated Pt/GaN and Pt/TiO_2 nanodiodes using shadow mask techniques. Early in the Project we decided to focus our efforts on the GaN based diodes because our ability to reproducibly dope this material over a wide range (as compared to TiO_2). A planar diode structure was designed (see Fig. 2) using GaN on sapphire as the substrate. The GaN films were grown by MOCVD on c-plane sapphire wafers to a typical thickness of ~3 microns. The films could be moderately doped with silicon (using silane) to yield n-type carrier concentrations of 2 X 10^{17} cm^{-3}, or heavily doped to ~5 X 10^{18} cm^{-3}. For some samples a thinner unintentionally-doped (uid) film was grown as the top layer, and exhibited a carrier concentration < 10^{16} cm^{-3}.

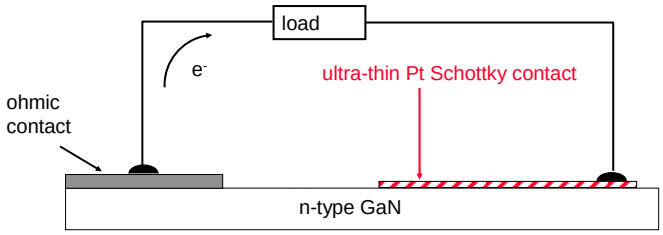

Figure 2. Schematic of a catalytic nanodiode (Schottky diode) device structure.

We originally processed 7-8 devices already diced into 6 X 12 mm pieces, but eventually moved to whole-wafers, followed by dicing, which led to a more reproducible process. The shadow mask set used for the whole-wafer processing also let us vary the Pt area and configuration (see Figure 3). Most devices were fabricated with Pt thickness of 5 nm.

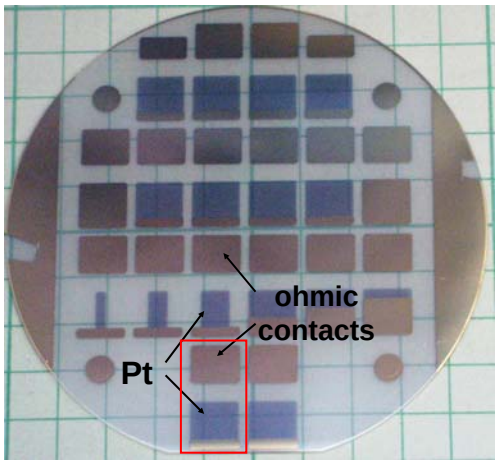

Figure 3. Processed (undiced) 5 nm Pt/GaN diodes on 2" sapphire wafer

Proper preparation of the GaN surface before Pt deposition was found to be critical for good diode performance. Early diodes suffered from poor rectification and high reverse bias leakage, typically milliamps at -1V. We eventually found that an oxygen ashing step followed by a buffered oxide etch (BOE) step just before Pt deposition led to near ideal diode performance and reverse bias leakages in the nanoamp range (with uid GaN, 5 nm Pt), as shown in Figure 4.

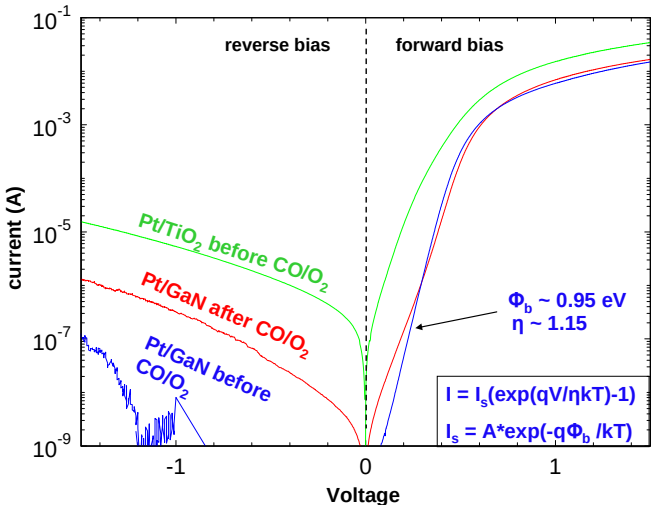

Figure 4. I-V behavior of Pt/GaN (uid) and Pt/TiO2 nanodiodes at room temperature

3. Search for chemicurrent

For the chemical-to-electrical tests we built a small vacuum system with a gas-handling system capable of handling CO and O_2. Diodes were mounted on a BN heater with the

appropriate electrical contacts (see Fig. 5). In early tests we only monitored the heater temperature, but we later added two thermocouples to the electrical contacts and also monitored the Pt surface temperature with a pyrometer (discussed in Section 4). The heater was capable of heating the samples well above 300°C, but most experiments were performed in the 200-300°C range.

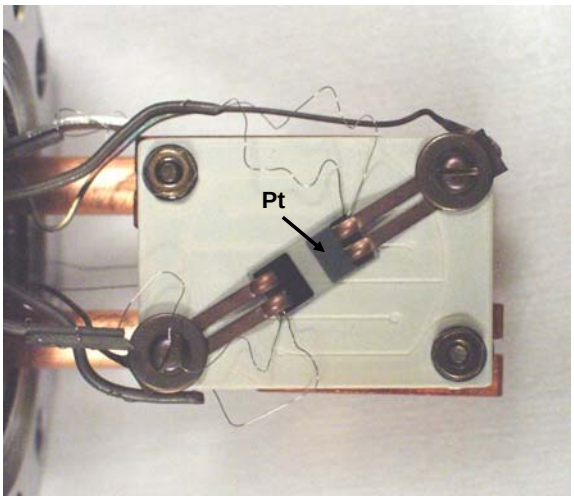

Figure 5. Pt/GaN nanodiode mounted on BN heater

Typical experiments were done in a "batch" mode, starting with ~100 Torr of O_2. A few Torr of CO was then added to the chamber, and the $CO + ½ O_2 \rightarrow CO_2$ reaction was run to completion. In early experiments we had difficulty finding evidence of "chemicurrent" because we were adding too much CO to the system, and the reaction rate becomes negative-order in P(CO) at high values [6], as shown schematically in Fig. 6a. We eventually found conditions where we could reliably generate an electrical signal indicative of the catalytic reaction, although as we will later show that it is not true chemicurrent. One example is shown in Fig. 6b, where the reaction occurs on 5 nm Pt at 270°C. The total pressure (red curve) in this figure is recorded while ~4 Torr of CO are added to the system. During this part of the experiment the current rises nearly linearly at first, then drops extremely rapidly at the kinetic phase transition **1** and is nearly constant for the next ~400 seconds. During this portion of the experiment the total pressure drops nearly linearly while CO is being consumed at a turnover frequency (TOF, or molecules per site per sec) of 70. At a sufficiently low CO partial pressure the system undergoes a 2nd kinetic phase transition (labeled **2** in Fig. 6a & b) and the current rises sharply to 510 nA. The

reaction rate also jumps up to TOF = 430. Beyond this transition the current and pressure fall nearly exponentially, as expected for a 1st-order rate process.

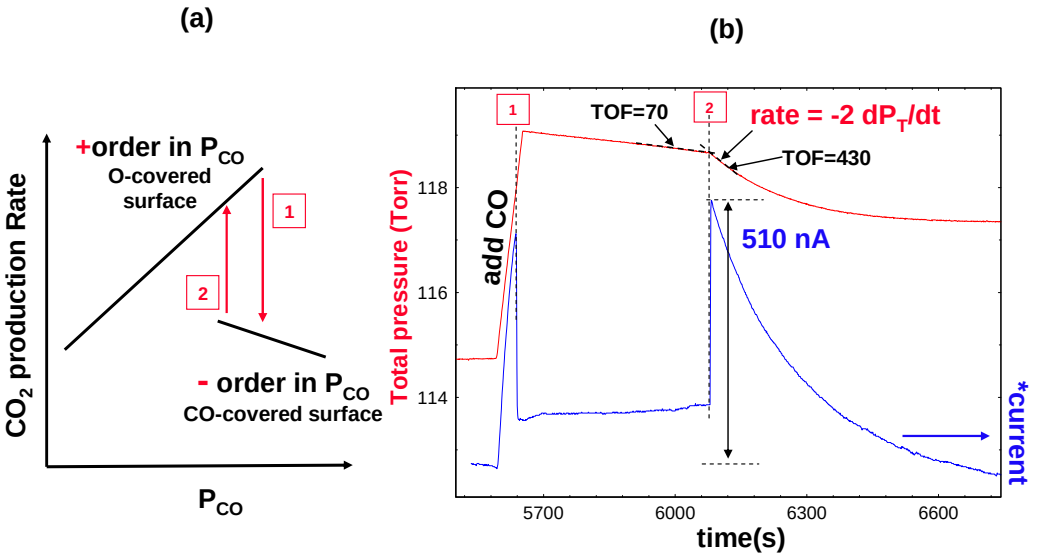

Figure 6. (a) schematic of CO oxidation kinetics as function of CO partial pressure, showing the 1st order to negative-order kinetic phase transition. (b) "chemicurrent" (blue line) and total pressure transient (red line) observed during CO oxidation on a 5 nm Pt nanodiode at 270°C. (*We are using the solar cell convention for the sign of the current)

We have performed a large number of experiments that all show this qualitative behavior with 2 kinetic phase transitions, exhibiting 2 peaks in the "chemicurrent" signal. We note that if too much CO is added to the system (e.g., > 10 Torr) it may take a very long time (e.g., hours) before the 2nd kinetic phase transition occurs.

As noted in Fig. 6b, we are measuring the absolute reaction rate by monitoring the total pressure and computing the slope. Dividing the electrical current by the reaction rate gives the "quantum yield" (Y) of the nanodiode, i.e., Y = electrons/CO_2 produced. Our initial results were very disappointing, with Y in the 10^{-5}-10^{-6} range. By drawing analogies to solar cells and photodiodes, we first speculated that perhaps most of the current was flowing through a parasitic shunt resistance (R_{sh}) and bypassing the current amplifier (see Fig. 1b). By changing R_{sh} we were able to eventually achieve yields near 10^{-3}. Our results spanning a year of effort are shown in Figure 7, and are compared to the results from Somorjai's group [1-5]. Our best yield results are still ~4 orders-of-magnitude below the early (2005) Somorjai reports of 0.75. However, it

appears that Somorjai's group has also been unable to reproduce the phenomenal results published in 2005, and their recent results are more closely matched to our results.

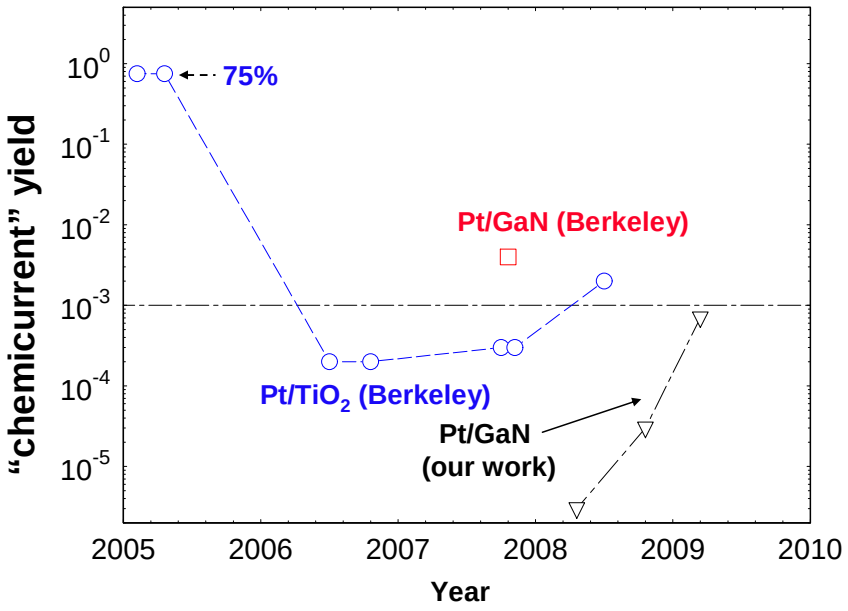

Figure 7. Yield measurements from Somorjai's work (ref. 1-5) compared to our results.

For our anticipated micropower applications a yield of ~10^{-3} is too low to be useful, and unfortunately we see no path forward that would substantially increase it. In fact, the prognosis is even worse, because at the midway point of the Project we became very skeptical of the whole notion of "chemicurrent". Referring back to Fig. 1b, for a true current source increasing the shunt resistance (R_{sh}) should eventually lead to an increase in the current flowing through the detector (R_L). If the signal is instead derived from a voltage source, increasing R_{sh} will eventually cause the detected current to decrease. In fact, the increases in Y noted in Fig. 7 were achieved by **lowering** R_{sh}, which is just the opposite trend expected for a current source. This effect is shown in more detail in Figure 8, where the peak current is plotted as a function of R_{sh} and R_L. When $R_L << R_{sh}$ the measured current is proportional to $1/R_{sh}$. This behavior is indicative of a voltage source, and is in semi-quantitative agreement with predictions using 0.25 mV (solid lines in Fig. 8) where both R_{sh} and R_L are accounted for.

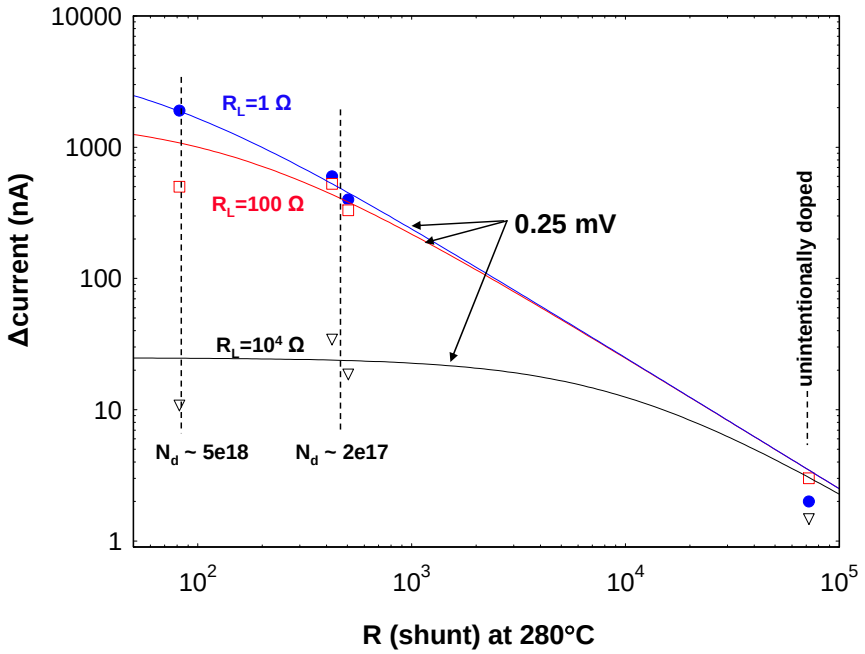

Figure 8. Current as a function of R_{sh} at various values of R_L. Solid lines are the predicted current from a voltage source of 0.25 mV.

The results displayed in Figure 8 are strong evidence that the electrical currents we measured are not due to true "chemicurrent", but are instead derived from a voltage source. The next obvious question is what is the nature of the voltage source, and why does it respond to the chemical reaction? As noted by Somorjai et al., there is usually a significant "baseline" current measured even without the chemical reaction, and they ascribe this feature to a thermoelectric current. We observe similar effects, and became suspicious that the thermoelectric voltage might also be responsible for the measured chemical signals, due to the exothermic nature of the chemical reaction. This lead to the final phase of this Project, where we both calculated and measured the temperature rises and gradients in the nanodiode (see next Section).

4. Modeling and experimental measurements of temperature gradients

As noted in the previous section, it only takes a small voltage source (~0.25 mV) to generate the observed electrical signals. Due to the large Seebeck coefficient for n-type GaN (~400 μV/K) [7], a relatively small temperature gradient (~1°C) between the electrical contacts

is sufficient to generate the observed currents. Park, et al. only considered temperature gradients within the thin metal and semiconductor layers, and concluded that the thermal effects of reaction exothermicity were small ($<10^{-3}$ °C) and could be neglected [5]. However, their model neglects the thermal resistance of the much thicker substrate wafer (e.g., sapphire) and the contact to the heater, and therefore substantially underestimates the surface temperature rise due to chemical reaction.

We have developed a more complete 1D model of the system, which is shown schematically in Figure 9. For this model we account for the four largest thermal resistances; the thermal contact resistance between the heater and the sapphire wafer (R_{cont}), the thermal resistance of the sapphire wafer (R_{sapp}), the thermal resistance due to radiation (R_{rad}), and the thermal resistance due to convection (R_{conv}). The latter three values may be reliably calculated

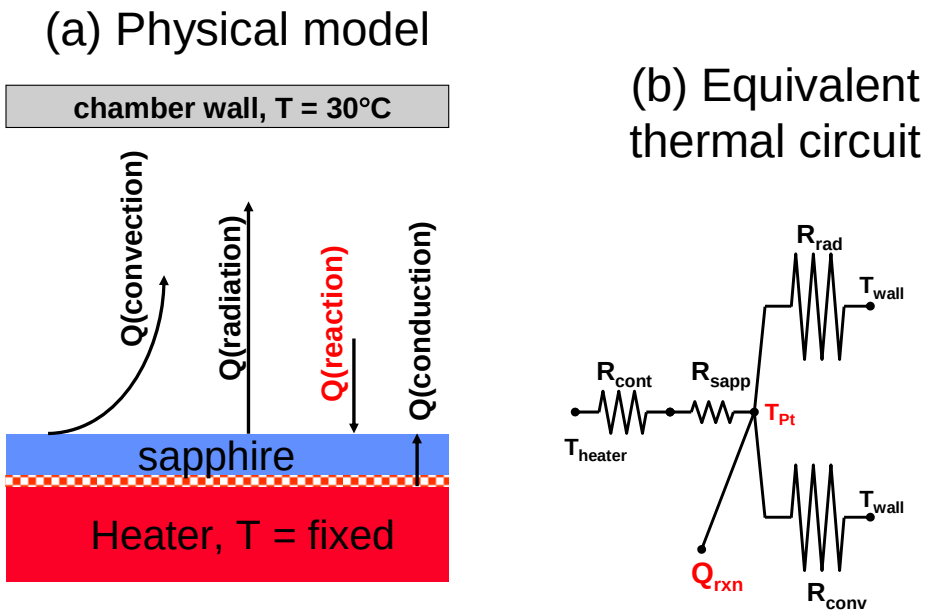

Figure 9. Schematic of 1-D thermal model

using the physical properties and dimensions of the materials. We have estimated the first resistance (R_{cont}) from pyrometric measurements of the temperature offsets between sapphire wafers and carriers during GaN MOCVD. The thermal resistance of the semiconductor (GaN)

and Pt film are orders-of-magnitude smaller and can be neglected in this analysis. The effect of the exothermic chemical reaction is accounted for by adding an extra heat source term (Q_{rxn}) at the Pt surface. The calculated temperature rise of the Pt surface as a function of Q_{rxn} assuming isothermal boundary conditions (T_{heater}=275 °C, T_{wall}=30 °C) is shown in Figure 10. At 300 mW/cm^2 (corresponding to a TOF ~400) the Pt surface temperature rise is 1.5°C, which is more than 3-orders-of-magnitude larger than the value estimated by Park, et al. [5].

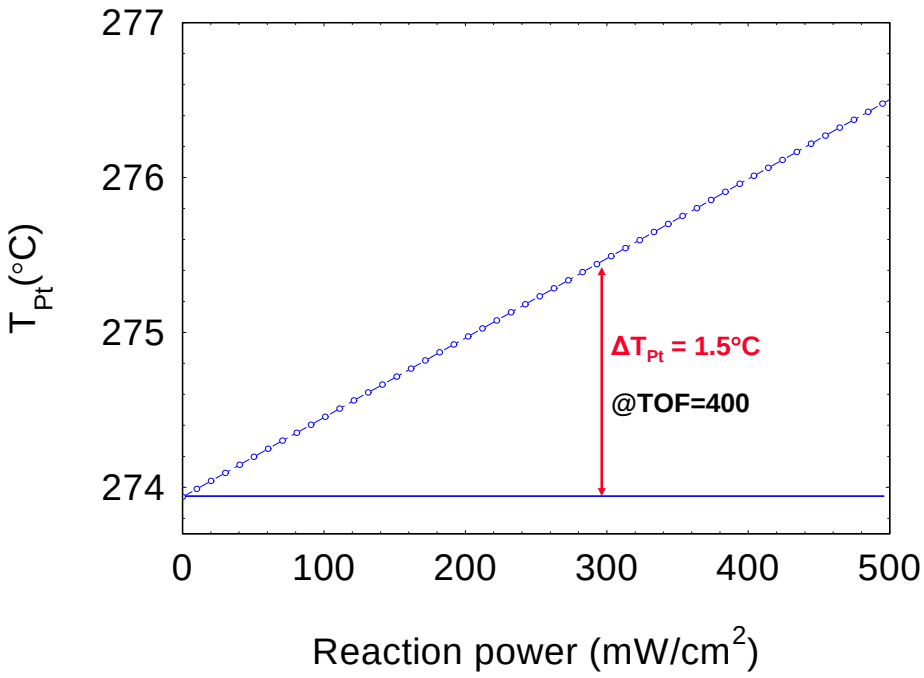

Figure 10. Pt surface temperature as a function of reaction power

If the lateral temperature gradient between the two electrical contacts is also of this magnitude, then it is more than sufficient to explain the observed thermoelectric current. To calculate this gradient requires a much more sophisticated 3D model of the system. For this task we employed a large-scale parallel device simulation code known, Charon [8]. Most of the physical details and dimensions of the reactor, heater, and nanodiode chip were included in the simulation, although the spring contacts used for electrical connections with the chip where omitted. The model accounts for conductive, convective, and radiative heat transfer. The heater and nanodiode chip under a steady-state reaction condition are shown in Figure 11, with the hottest (red) spot corresponding the to Pt area. An example of the lateral temperature profiles

across the chip before and during reaction is shown in figure 12. Without the chemical reaction (Q = 0) the ohmic contact is slightly hotter than the Pt contact, which is due to the lower emissivity (higher radiative resistance) of the ohmic contact. This initial temperature gradient is

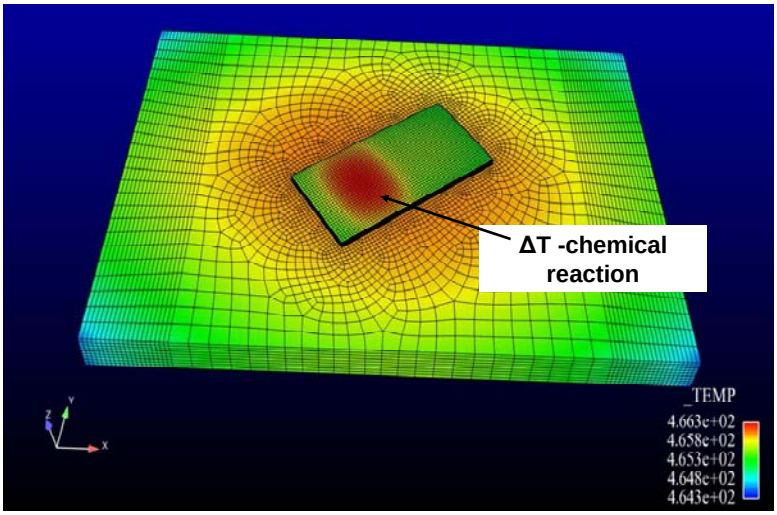

Figure 11. Full 3D result showing Pt temperature rise for a chemical reaction power of 300 mW/cm^2

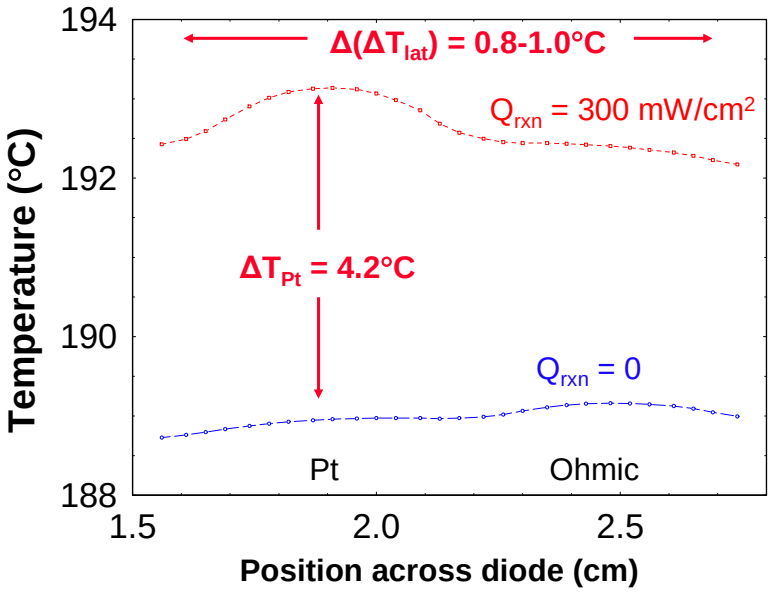

Figure 12. Lateral temperature profile across nanodiode chip with Q_{rxn} = 0 and 300 mW/cm^2

consistent with the sign of the baseline thermoelectric current we typically observe. When the reaction is turned on at Q_{rxn} = 300 mW/cm^2, the Pt surface temperature rises 4.2 °C. This temperature rise is larger than the 1D result described above mainly because the 3D model uses a constant heater power boundary condition, instead of an isothermal boundary condition. With the reaction turned on, the change in the lateral temperature gradient is 0.8-1.0 °C, depending on exactly where we define the electrical contact. As noted before, a value of ~1 °C is sufficient to produce the observed electrical signals.

In addition to the simulations described above, we also have made direct experimental measurements of the temperature changes. In order to measure the Pt surface temperature, we chose to use pyrometry, which is a non-contact and therefore non-perturbative method. The Pt layers are optically semitransparent, even in the infrared, so the choice of detection wavelength is important. The sapphire wafers are also transparent in the visible and infrared down to about 6-7 microns. Fortunately, from previous work we had developed a mid-infrared pyrometer with a detection wavelength of 7.5 microns [9]. At this wavelength sapphire is optically opaque with an emissivity > 0.95, and both CO and CO_2 are transparent. The high value of the sapphire extinction coefficient at this wavelength means that we are essentially probing the surface temperature.

Two important modifications were made to the pyrometer design. First, the optical path was redesigned to yield a smaller detection area on the chip surface, with a diameter of 2-3 mm (Pt dimension is typically 4 X 5 mm). Second, a collinear white light source was injected into the optical path so we could visually inspect the spot we were measuring. The pyrometer signal was then calibrated against the heater thermocouple. This likely introduces an absolute error of a few degrees, but since we are mainly interested in temperature **changes** the relative error is very small. Results from a typical experiment are shown in Fig. 13. Note that the peak temperature rise of 2.6 °C is in good agreement with our 1D and 3D simulations. Also note the strong correlation between the Pt surface temperature and the measured electrical current.

In order to measure the lateral temperature gradient we inserted a fine-wire type K thermocouple under an electrical contact on each side of the chip (see Fig. 5). The temperature difference (T_{Pt}-T_{ohmic}) during an experiment is plotted in Figure 14. The peak experimental value is somewhat lower than the 3D simulation, but it is still sufficient to explain the electrical

measurements. In fact, we can predict the current using the GaN Seebeck coefficient (S = -400 μV/deg), the measured temperature change (ΔT), and the diode resistance (R); $\Delta i = S \cdot \Delta T/R$.

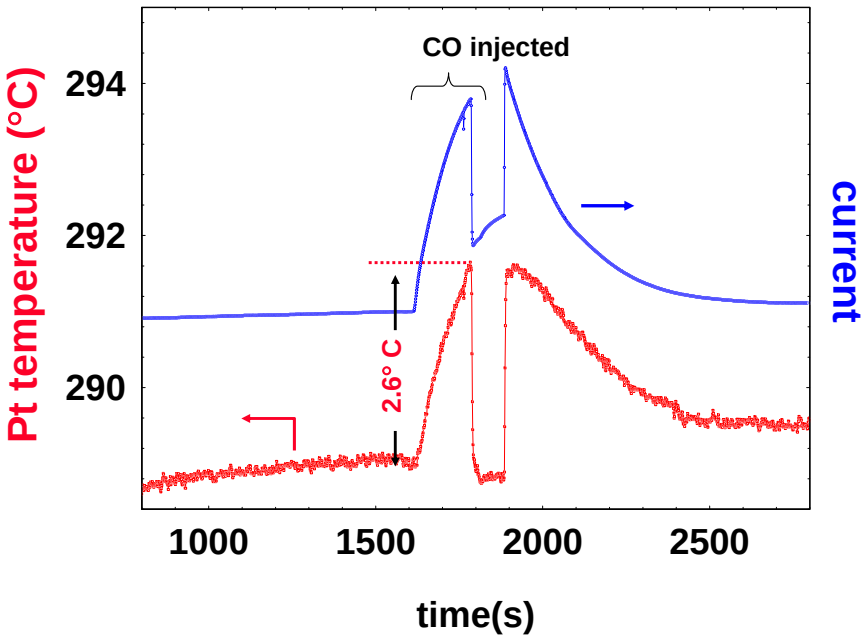

Figure 13. Pt temperature (red) measured with mid-IR pyrometer compared to electrical current (blue)

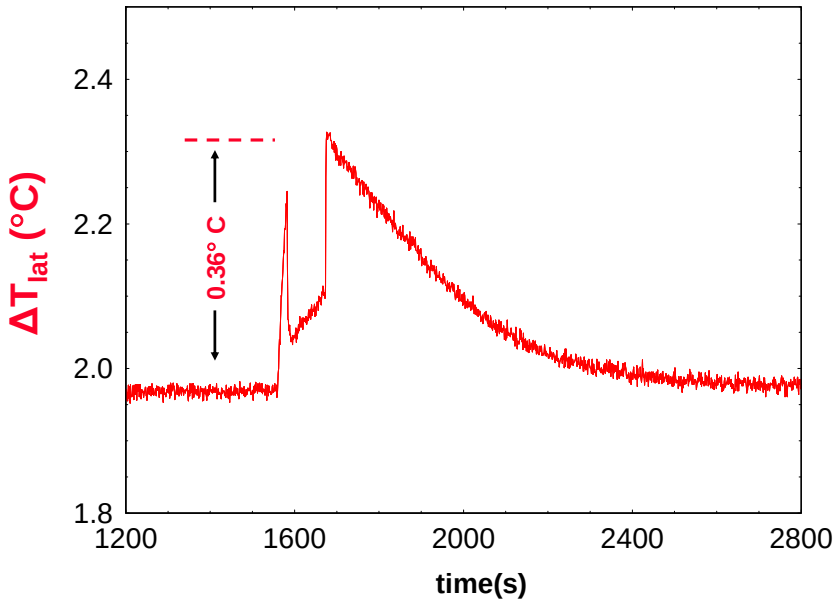

Figure 14. Lateral temperature difference (Pt-ohmic) measured by thermocouple

The predicted current is overlaid with the measured current in Figure 15. The two curves have been shifted to yield a common baseline, but they are on the same absolute current scale. The predicted thermoelectric current displays all of the qualitative features and is in near perfect quantitative agreement over the entire experiment.

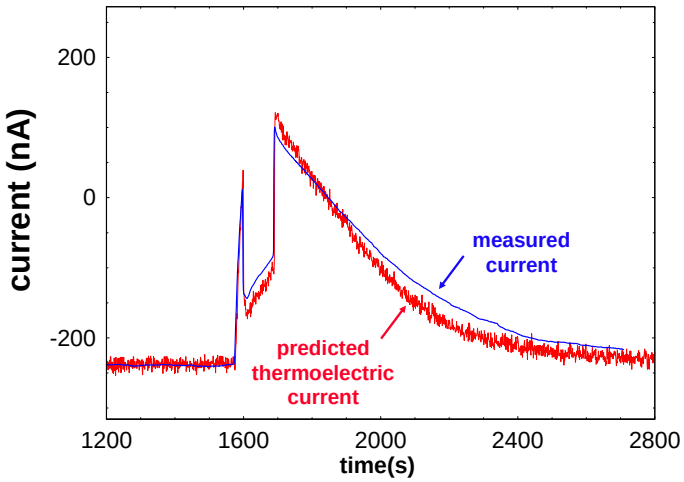

Figure 15. Comparison of the measured current and the predicted thermoelectric current

4. Summary

We have fabricated and tested a large number of Pt/GaN nanodiode devices under CO oxidation conditions. We have measured electrical currents up to several microamps, and reaction yields (electrons/CO_2) up to ~10^{-3}. These results are in reasonable agreement with more recent results for Somorjai's group. We were unable to achieve anything near the 75% yield first reported by Somorjai, but apparently they have not been able to reproduce this result either.

In an unexpected turn of events, midway through this Project we began to question whether the measured current was true chemicurrent, or instead simply due to a thermoelectric voltage generated by the exothermic chemical reaction. The first clue was that the measured current didn't scale with the diode shunt resistance in a way consistent with a current source. The current instead behaved as if it were coming from a voltage source. The likely candidate was a thermoelectric voltage generated by a small temperature gradient (~1 °C), in concert with the large Seebeck coefficient for n-type GaN (-400 μV/deg). Given the likely controversial nature of this assertion, the last year of the Project was focused on calculating and measuring the

temperature changes in the diode during chemical reaction. Our results conclusively demonstrate that the current we measure from our nanodiodes is derived from the thermoelectric voltage; we have found no credible evidence for true chemicurrent. Unfortunately this means that the catalytic nanodiode has no future as a micropower source.

5. References

[1] Z.J. Xiao and G.A. Somorjai, J. Phys. Chem. B 109 (2005) 22530.
[2] J. Xiaozhong, A. Zuppero, J.M. Gidwani, and G.A. Somorjai, J. Amer. Chem. Soc. 127 (2005) 5792.
[3] J. Xiaozhong, A. Zuppero, J.M. Gidwani, and G.A. Somorjai, Nano Letters 5 (2005) 753.
[4] J.Y. Park and G.A. Somorjai, J. Vac. Sci. Technol. B24 **(** 2006) 1967.
[5] J.Y. Park, J.R. Renzas, A.M. Contreras, and G.A. Somorjai, Top. Cat. 46 (2007) 217
[6] J.R. Creighton, F.-H. Tseng, J. M. White, and J. S. Turner, J. Phys. Chem. 85 (1981) 703
[7] our measurement, note that TiO_2 is similar, also see M. S. Brandt, P. Herbst, H. Angerer, O. Ambacher, and M. Stutzmann, Phys. Rev. B (1998) 7786.
[8] http://www.cs.sandia.gov/newsnotes/2005newsnotes.html#Charon
[9] J.R. Creighton, W.G. Breiland, D.D. Koleske, G. Thaler, M.H. Crawford, J. Crystal Growth, 310 (2008) 1062.

Distribution

MS 0359	LDRD office, 1911
MS 1086	J. R. Creighton, 1126
MS 1086	M. E. Coltrin, 1126
MS 1318	R. P. Pawlowski, 1414
MS 1086	R. M. Biefeld, 1126
MS 0899	Technical Library, 9536 (electronic copy)


Sandia National Laboratories